# UNIVERSITY OF BIRMINGHAM

## University of Birmingham
## Research at Birmingham

# A heat perturbation flow meter for application in soft sediments

Greswell, Richard; Riley, Michael; Alves, PF; Tellam, John

Link to publication on Research at Birmingham portal

# A heat perturbation flow meter for application in soft sediments

Richard B. Greswell, Michael S. Riley *, Patricia Fernandes Alves [1], John H. Tellam

Hydrogeology Research Group, School of Geography, Earth and Environmental Sciences, University of Birmingham, Edgbaston, Birmingham B15 2TT, UK

## ARTICLE INFO

## SUMMARY

A prototype flow meter has been developed, based upon the heat perturbation principle, to monitor groundwater specific discharge in soft sediments. The device is designed for use in spatially intensive, long-term monitoring campaigns in remote or inconvenient locations, and is cheap, robust and capable of being logged automatically. The results of the laboratory tests indicate that the heat perturbation principle is suitable for determining the magnitude of specific discharge to a degree of accuracy that would be useful in practical applications in dynamic groundwater systems with rapidly changing flows of approximately 1 md$^{-1}$ or more and that the groundwater flow direction can generally be determined to a high level of precision. The accuracy and reliability of the estimates of specific discharge have been shown to depend strongly upon the geometrical precision of manufacture and the quality of the temperature monitoring system. These factors become most significant in the estimation of lower flows and further investigation is required to determine the detection limit of the device. Specific discharge estimates have been shown to be insensitive to dispersivity values appropriate to the scale of the device. Unlike the majority of heat perturbation devices, calibration is unnecessary.

## Introduction

Detailed, and often small scale, investigations into the movement of groundwater-borne contaminants play an important rôle in the assessment of economically and environmentally sensitive activities, such as the redevelopment of contaminated land sites, the remediation of contaminated groundwater, the identification of sources of groundwater pollution, and the evaluation of natural attenuation in highly heterogeneous media such as riparian and riverbed sediments. Such investigations demand the ability to monitor groundwater specific discharge intensively, often at spatial and temporal scales inappropriate for the application of traditional indirect methods based upon head and permeability measurements, or more direct determinations using borehole point dilution techniques. The variability of flow and the all too frequent need to monitor in remote and inconvenient locations present substantial technical challenges to the development of suitable measurement devices. In order to accommodate the need for spatially intensive, long-term monitoring in heterogeneous sediments, in remote locations, monitoring instrumentation needs to be inexpensive, compact and robust, with a data logging capability and a low power requirement. To date, the development of small-scale

flow monitoring devices has been centred largely on determining the magnitude of groundwater specific discharge, principally in a predetermined direction. In this paper we outline the design, construction and laboratory testing of a prototype device, or probe, to measure both the magnitude and direction of specific discharge in two dimensions that satisfies the requirements listed above.

The probe is based upon the heat perturbation method, which is a technique exploited extensively in its one-dimensional form in borehole logging and soil science applications (e.g. Dudgeon et al., 1975; Greswell, 2005). The underlying principle is straightforward. A heater and, in two dimensions, a surrounding array of temperature sensors are embedded in a groundwater-saturated porous medium. The heater is switched on for a short period and the consequent changes in temperature at the sensors recorded. The magnitude and direction of the specific discharge of the groundwater has a strong influence on the development of the heat plume, and can be estimated from the resulting temperature changes.

Precursors of this kind of probe were developed initially to provide a simple way to measure the thermal properties of soil in which water flow was insignificant. Campbell et al. (1991) constructed a device consisting of two needle-like probes, one a heater and the other a temperature sensor, which became known as the dual-probe heat pulse sensor (DPHP). Later workers such as Welch et al. (1996), Bristow (1998), Heitman et al. (2003) and Basinger et al. (2003) refined both the technique and the analysis and provided further evaluation of the approach in both laboratory and

---

* Corresponding author. Tel.: +44 (0)121 414 6163; fax: +44 (0)121 414 4942.
  E-mail address: M.Riley@bham.ac.uk (M.S. Riley).
[1] Present address: WS Atkins plc, Woodcote Grove, Ashley Road, Epsom, Surrey KT18 5BW, UK.

field environments. Using solutions taking into account heat conduction and convection it was shown that the device could accurately measure the volumetric heat capacity, thermal diffusivity, and volumetric water content of unsaturated soils. Ham and Benson (2004) proposed optimised parameters for the design, calibration, and operation of DPHP sensors.

Subsequently, the heat perturbation principle was used to estimate groundwater flow in one dimension given that the thermal properties of the sediment could be estimated either independently or by first engineering zero flow conditions in the field. This was achieved by Ren et al. (1999) who modified the DPHP to include a second temperature sensor positioned at the same distance on the other side of the heater as the first and in a common plane. Ren et al. (2000) were then able to estimate water flux using the maximum (dimensionless) temperature difference (MDTD) between the probes. Using a column filled with different fully saturated soil types, flows were estimated reasonably well using the technique over a range of imposed fluxes, although the error between estimated and actual flow increased with increasing flux and decreasing grain size. Mori et al. (2003) developed a similar multi-function device and performed a limited number of saturated flow experiments, the findings of which were similar to Ren et al. (2000) insofar as flows were underestimated in the same manner for similar sediment types. The low flow limit, based on experimental data, was placed at about 0.7 md$^{-1}$. Hopmans et al. (2002) analysed the data from a similar device using inverse numerical modelling that included the physical size of the needles and a thermal dispersivity term.

The complexity of the numerical solution approach of Hopmans et al. (2002), although later simplified by Knight and Kluitenberg (2004), led to the development of a solution by Wang et al. (2002) based on the relationship between the water flux, the natural logarithm of the ratio of the temperature difference of the sensor probes and the (predetermined) thermal conductivity of the sediment. The method was evaluated by Ochsner et al. (2005) who found that it compared favourably with the MDTD approach. However, for both methods there proved to be a significant underestimation of flux, which as had been found by Ren et al. (2000), proved worse for finer grained sediment, but which was still significant for sands. Gao et al. (2006) conducted experiments to demonstrate the error to be attributable to wall effects creating an annular zone of high permeability due to a lower packing density of the sediment at the edges of the experimental cylinder, but it is interesting to note that Ren et al. (2000) sealed the annulus between the sample and the test cylinder with wax and yet still reported unexplained underestimation of flux.

Heat perturbation devices have been developed to determine the groundwater flow direction and as well as magnitude. The Geoflo system, manufactured by Kerfoot Technologies Inc., and summarised by Wilson et al. (2001) is designed to measure horizontal flows. This device employs a heater surrounded by an even number of temperature sensors, and is embedded in an artificial porous medium comprising silica beads, which can be installed in a borehole and held in place using a purpose built packer or installed directly into unconsolidated sediments. The magnitude of the groundwater velocity is determined from the difference in temperature changes between diametrically paired sensors, and the flow direction is determined by considering these velocities as components of the actual velocity. Laboratory-based calibration is required to characterise the response of the device, and since the permeability and porosity of the silica bead medium and its packer will in general be different from those of the aquifer, suitable corrections based upon the aquifer properties have to be made to the velocity measured in the device to give the water velocity in the aquifer. Guaraglia and Pousa (2007) investigate a method to improve the quality of the inferred flow direction by

including more temperature sensors, but find a consequent reduction in the accuracy of the flow rate.

Ballard (1996) developed a probe consisting of a cylindrical heater about 75 cm long by 5 cm in diameter with an array of 30 calibrated temperature sensors located on their surface. The probe is emplaced permanently in the aquifer using a hollow stem auger. The temperature of the sediment and groundwater surrounding the probe is then increased by 20–30 K by a 100 W heater over several hours. The magnitude and direction (in three dimensions) of the groundwater velocity, and the thermal properties of the sediment are determined by fitting a mathematical model of the temperature distribution on the cylinder surface using the simplex optimisation method. Correction factors have to be applied to take account of the period in which thermal gradients are established within the cylinder. Su et al. (2006) suggest that the variability in thermal properties of the aquifer over the length of the probe may produce anomalous vertical discharges.

In style, the probe described in this paper is a further development of the modifications to the DPHP described by Ren et al. (1999) and Mori et al. (2003), and consequently is small (measurements are averaged over a volume of less than 10 cm$^3$) with a low power requirement, but has been extended to measure the magnitude and direction of flow in two dimensions. As in the device of Ballard (1996), the analysis of the output is achieved using an optimisation routine to estimate parameter values of a mathematical model, which allows the simultaneous determination of the magnitude and direction of the groundwater specific discharge and robust estimation of the thermal properties of the saturated sediments in which it is installed, obviating the need for calibration in the field. In addition, since the device is small, the risk of observing fictitious flows due to spatial variability in the sediment thermal properties is minimised. In contrast to the Geoflo system, the heater and temperature sensors in the probe are in direct contact with the sediment, and so there is no need to have knowledge of and make corrections for the sediment permeability.

## The probe design

### Overview

The probe is shown diagrammatically in Fig. 1. It consists of three main elements: a heater; a set of temperature sensors; and an ABS (acrylonitrile butadiene styrene) support block. The four temperature sensors (diameter 1.61 mm and length 30 mm) are installed in the support block (diameter 30 mm), equidistant from each other around a circle of radius 6 mm and referred to here as N, S, E and W. The heater (diameter 1.61 mm and length 35 mm) is located at the centre of the circle. Details of the design of the
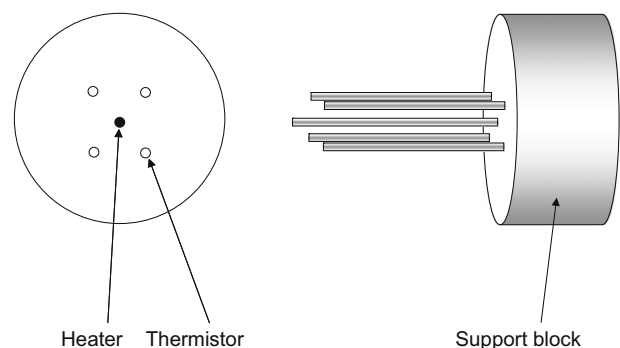


**Fig. 1.** Probe design showing central heater surrounded by four equally spaced temperature sensors embedded in an ABS plastic block.

heater and temperature sensors are given in the following subsections.

The heater and temperature sensors were press-fitted into holes drilled into the columnar block of ABS, which has a low thermal conductivity (approximately 0.25 Wm$^{-1}$ K$^{-1}$) and volumetric heat capacity (approximately $1.5 \times 10^6$ Jm$^{-3}$ K$^{-1}$), which minimises its potential to act as a heat sink, thereby avoiding the sources of error outlined by Ham and Benson (2004). The wires from the heater element and sensors were soldered to a multi-core cable before the exposed conductors were encapsulated in a polyurethane resin that covered both the cables and the rearmost portion of the support block.

*The heater*

Following proposals by Campbell et al. (1991), heaters in previous studies have typically been constructed using a stainless steel hypodermic needle with an internal diameter sufficient to take a heater element comprising loops of enamelled (insulated) electrical resistance wire such as nichrome. Following emplacement, the heating wire has then usually been sealed into place using a high conductivity epoxy resin such as 'Omegabond 101' (Ham and Benson, 2004) which has a thermal conductivity of approximately 1.0 Wm$^{-1}$ K$^{-1}$ and facilitates the transfer of heat from the element to the heater casing and also seals the cavity from the ingress of water. In the design described here, attempts were made to improve the thermal properties of the heater unit. First, the heater element was constructed by winding a coil of 0.08 mm diameter enamelled NiCr wire around a glass fibre (Fig. 2 'A') to produce a coil that had a resistance of 34 Ω. In this way the distribution of the wire was controlled and evenly spaced to produce a more uniform heating pattern. Second, the heat transfer from the element to the heater casing was enhanced by injecting a zinc oxide based heat transfer compound (RS components part no. 217-3835; thermal conductivity = 2.9 Wm$^{-1}$ K$^{-1}$) to encapsulate the heater. Finally, a small brass plug (Fig. 2 'B') was pressed into the end of the needle ('C') to act as a seal.

*Temperature sensors*

Previous workers have used either small thermocouples or thermistors to measure the temperature changes. Thermistors

are typically configured as one element within a resistance or Wheatstone bridge. Since the resistance of a thermistor is temperature-dependent, any change in temperature will produce a voltage at the point of measurement. Compared with that produced by thermocouples, this voltage is large, and when combined with sensitive data-loggers or other instruments, this allows the temperature to be resolved to about 0.001 K (Ham and Benson, 2004). In this study, thermistors were used, but the resolution was limited by the analogue–digital interface of the logger to approximately 0.01 K. The larger signal produced by thermistors also provides better protection against noise induced in the system from external electrical devices.

Mini BetaCURVE Probe thermistors manufactured by Betatherm (Fig. 2 'D') were chosen in this study because of their small size (0.5 mm diameter), which allowed them to be installed within the needles, and for their close manufacturing tolerances, which promote the production of identical temperature/resistance curves for all individual devices. These thermistors were placed within hypodermic needles identical to that used for the heater and encapsulated and sealed in the same way.

*Electrical configuration*

Power for the heater and the sensor bridges is supplied from a single 12 V battery, which is regulated to supply a stable voltage for the sensor bridges and the heater element via an adjustable voltage regulator, which allows the power input to the probe to be varied. The bridges were constructed using 10 kΩ precision, high stability, wire-wound resistors manufactured by Neohm. Measurement of the heater power was achieved using an in-line ammeter and a voltmeter. During the experiments, the output voltage from the bridge was monitored using a DaqPro 5300 data logger, which has a 12 bit resolution.

## Mathematical analysis

*The heat balance equation*

Analysis of the output from the probe is based upon the equation describing the transport of heat in a two-dimensional saturated porous medium with fluid flow along the $x$-axis, namely

$$\frac{\partial T}{\partial t} = D_L \frac{\partial^2 T}{\partial x^2} + D_T \frac{\partial^2 T}{\partial y^2} - u \frac{\partial T}{\partial x} + \frac{Q}{(\rho C)_m} \tag{1}$$

where $T$ is the temperature of the saturated medium (K); $u = \frac{(\rho C)_f}{(\rho C)_m} q$ is a thermal advective term (ms$^{-1}$); $(\rho C)_f$ is the volumetric specific heat of the fluid (Jm$^{-3}$ K$^{-1}$); $(\rho C)_m$ is the volumetric specific heat of the saturated medium (Jm$^{-3}$ K$^{-1}$); $q$ is the magnitude of the groundwater specific discharge (ms$^{-1}$); $D_L$ and $D_T$ are the longitudinal and transverse heat dispersion coefficients, respectively (m$^2$ s$^{-1}$) given by $D_L = \alpha_L u + \lambda$ and $D_T = \alpha_T u + \lambda$; $\alpha_L$ and $\alpha_T$ are the longitudinal and transverse dispersivity, respectively (m); $\lambda = \frac{\kappa_m}{(\rho C)_m}$ is the thermal diffusivity of the saturated sediment (m$^2$ s$^{-1}$); $\kappa_m$ is the magnitude of the (assumed isotropic) thermal conductivity (Wm$^{-1}$ K$^{-1}$) of the saturated medium and $Q$ is the spatially variable rate of addition of heat energy per unit area per unit thickness (Wm$^{-3}$) of saturated medium.

*Solutions of the heat balance equation*

For an input of heat at the origin in an infinite medium during the time interval from $\tau$ to $\tau + \Delta\tau$ and at a rate $Q'$ Watts per metre thickness of sediment, the resulting temperature rise, $\Delta T$, as a function of space and time can be derived from Eq. (1), and is given (adapting results from Carslaw and Jaeger, 1959 and Bear, 1979) by
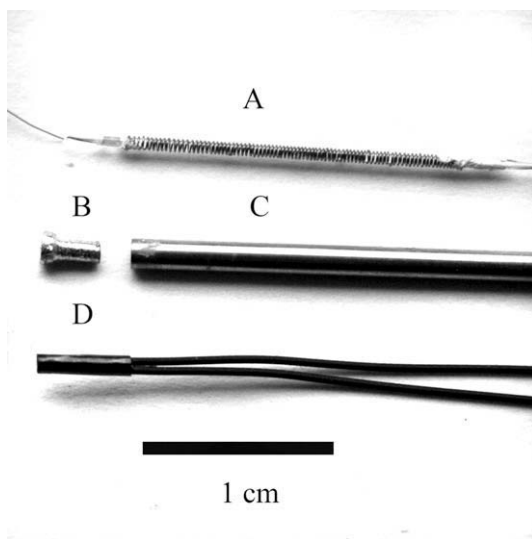


Fig. 2. Photograph showing the components of the heater and temperature sensors.

$$\Delta T = \frac{T_0}{(t-\tau)} \exp\left[-\frac{(x-u(t-\tau))^2}{4D_L(t-\tau)} - \frac{y^2}{4D_T(t-\tau)}\right]\Delta\tau \qquad (2)$$

where

$$T_0 = \frac{Q'}{4\pi(\rho C)_m\sqrt{D_L D_T}} \qquad (3)$$

In the analysis of the output from the probe, the direction of flow is not known a priori and so in order to apply Eq. (2) to the data, the axes have to be rotated through an unknown angle, $\theta$, so that the $x$-axis is aligned with the flow direction in the field. In the following, $\theta$ is the angle between the field flow direction and the East sensor of the probe (measured clockwise). For a continuous source of heat at the origin, the temperature changes, $\Delta T_X$ [for $X = N, S, E, W$] at each sensor are given by integrating Eq. (2) with respect to time to give

$$\Delta T_E = \int_{\tau=0}^{\tau=t} \frac{T_0}{t-\tau} \exp\left[-\frac{(x_E\cos\theta - u(t-\tau))^2}{4D_L(t-\tau)} - \frac{(y_E\sin\theta)^2}{4D_T(t-\tau)}\right]d\tau$$
$$(4)$$

$$\Delta T_N = \int_{\tau=0}^{\tau=t} \frac{T_0}{t-\tau}$$
$$\times \exp\left[-\frac{(x_N\cos(\theta+\pi/2) - u(t-\tau))^2}{4D_L(t-\tau)} - \frac{(y_N\sin(\theta+\pi/2))^2}{4D_T(t-\tau)}\right]d\tau$$
$$(5)$$

$$\Delta T_W = \int_{\tau=0}^{\tau=t} \frac{T_0}{t-\tau}$$
$$\times \exp\left[-\frac{(x_W\cos(\theta+\pi) - u(t-\tau))^2}{4D_L(t-\tau)} - \frac{(y_W\sin(\theta+\pi))^2}{4D_T(t-\tau)}\right]d\tau$$
$$(6)$$

$$\Delta T_S = \int_{\tau=0}^{\tau=t} \frac{T_0}{t-\tau}$$
$$\times \exp\left[-\frac{(x_S\cos(\theta+3\pi/2) - u(t-\tau))^2}{4D_L(t-\tau)} - \frac{(y_S\sin(\theta+3\pi/2))^2}{4D_T(t-\tau)}\right]d\tau$$
$$(7)$$

where $(x_X, y_X)$ [for $X = N, S, E, W$] are the coordinates of the location of each of the four sensors using East and North as the $x$- and $y$-axes, respectively. Eqs. (4)–(7) apply for non-zero values of $u$. When $u$ is zero the solution to Eq. (1) is independent of $\theta$, and the trigonometric factors in Eqs. (4)–(7) have to be removed.

*Determining specific discharge and flow direction*

Parameter estimation can be achieved by fitting the model described by Eqs. (4)–(7) to the time series of temperature changes recorded at the sensors for each flow measurement independently. However, where repeated flow measurements have been made, as in the laboratory experiments described here or as would be the case in a field situation with a permanently installed probe, the thermal and hydrodynamic dispersive properties should be subject to no more than minor changes between measurements. In this case, it is appropriate to consider fitting the model to a sequence of measurements by constraining these properties to be the same for each measurement.

Model fitting can be accomplished using a simple, but robust optimisation routine implemented for test purposes using VBA in EXCEL. The integrals in Eqs. (4)–(7) are evaluated numerically, and the goodness of fit to the data measured by the RMS error. The full set of optimisation parameters comprises the magnitude,

$u$, and direction, $\theta$, of the thermal advective vector, the volumetric heat capacity, $(\rho C)_m$, and the thermal diffusivity, $\lambda$, of the saturated sediment, and the longitudinal and transverse dispersivity values, $\alpha_L$ and $\alpha_T$.

The flow direction can be determined simply from $\theta$, but the magnitude of the specific discharge is given by

$$q = \frac{(\rho C)_m}{(\rho C)_f} u \qquad (8)$$

Thus, the value of $(\rho C)_f$ for the groundwater, which is temperature-dependent, is required. Perry and Green (1997) give the heat capacity of pure water as a function of temperature in Kelvin as

$$2.7637 \times 10^5 - 2.0901 \times 10^3 T + 8.1250 T^2 - 1.4116$$
$$\times 10^{-2} T^3 + 9.3701 \times 10^{-6} T^4 \text{ J kmol}^{-1} \text{ K}^{-1} \qquad (9)$$

and the density at typical field and laboratory temperatures of 12 °C and 20 °C as 999.477 kg m$^{-3}$ and 998.204 kg m$^{-3}$, respectively. This gives $(\rho C)_f$ as $4.199 \times 10^6$ Jm$^{-3}$ K$^{-1}$ at 12 °C and $4.182 \times 10^6$ Jm$^{-3}$ K$^{-1}$ at 20 °C.

Since the thermal diffusivity, $\lambda$, is estimated from the optimisation process, a value for the thermal conductivity of the saturated sediment can be inferred from that and the estimated heat capacity if required.

### Laboratory experiments

*Experimental apparatus*

Performance of the probe was evaluated using flow systems of known magnitude and direction. This was achieved by placing the probe in a small cylindrical 'turret' attached at right angles to a 4.5 cm diameter × 30 cm poly(methyl methacrylate) (Plexiglas) column, filled with water-saturated sand (Fig. 3). The probe orientation was set by inserting it so that the $N$ and $S$ sensors were aligned at a given angle with marks on the long axis of the column. Each end of the column was sealed by an end plate containing a central tube allowing water to be introduced by a digitally controlled peristaltic pump at the base, with discharge at the top. After
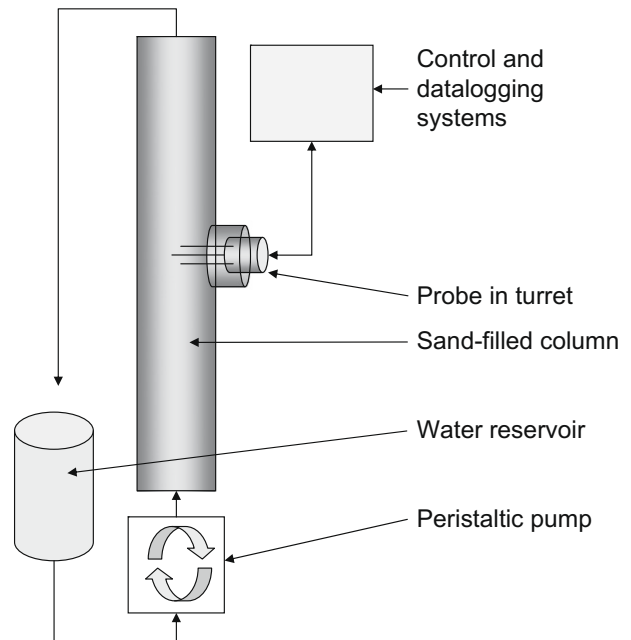


**Fig. 3.** Schematic diagram of the experimental apparatus.

sealing the probe into the turret in the desired orientation, the column was wet-packed with sand. Water from a reservoir was pumped through the column with the discharge returned to the reservoir. In order to minimise unwanted temperature variations, the column and static water supply were left to reach thermal equilibrium for 24 h prior to undertaking each set of experiments in a particular orientation.

### Experiment method

For each in a series of experiments, the probe was fixed in a set orientation and the desired flow rate set on the pump. After allowing a 30 min stabilisation period during which water was passed through the column and the power to the resistance bridge was applied, the logger was started. One minute later, power was applied to the heater for a 5 min period during which the voltage from the Wheatstone bridge of each probe was recorded every second. Without disturbing the probe, the experiment was then repeated at different discharge rates ranging from 0 to 5.9 ml min$^{-1}$ in six approximately equal steps. These rates are equivalent to specific discharges of 0–5.6 md$^{-1}$. The probe was then removed from the turret and, with the minimum of disturbance to the sand, replaced in a new orientation and the flow experiments repeated. For all experiments the bridge voltage and heater power were held constant at 10.16 V and 0.217 W, respectively. The typical maximum temperature increase recorded was less than 1 K.

## Results

### Initial data processing

Temperature change curves were constructed for each sensor relative to the recorded temperature at the time at which the heater was switched on. This approach was taken in order to simulate an automated process that would be required in a practical field application. However, the data from the temperature sensors is subject to noise and if the temperature recorded at the fixed start time happens to be unrepresentative of the true ambient temperature, the calculated temperature change curve will be shifted up or down by the magnitude of the deviation. Since the flow rate is related to the spread of the temperature change curves, shifting one or more of them up or down relative to the others will affect the estimated flow rate. Initial investigations showed that errors as small as 0.01 K in the ambient start temperature at just one sensor produced unacceptably large errors in the estimated flow rate. Hence, all data were pre-processed prior to construction of the temperature change curves by applying a median filter in which the temperature at time measurement $n$ is replaced by the median of the temperature from time measurement $n - 2$ to $n + 2$ inclusive. The application of this filter has the added advantage of smoothing the optimisation objective function, thus improving the quality of the optimisation routine.

### Effective distances between the heater and sensors

Initial modelling showed the estimates of specific discharge to be sensitive to the locations of the sensors. The reason for this sensitivity lies in the small distance between the sensors and the heater (nominally 6 mm). Measurements of the exact locations of each sensor were hampered by small but potentially significant deviations in their alignment, and so the effective distance of each sensor from the heater was estimated by conducting an experiment under no flow conditions by embedding the probe in an agar gel, which has the thermal properties of water. Eqs. (4)–(7) were then applied to the monitored temperature rise at each sensor to find

the optimised distances between the sensors and the heater (North 6.00 mm; South 5.99 mm; East 6.00 mm; and West 5.60 mm). This procedure does not give the deviations of the sensor locations from North, South, East or West, which were taken to be zero in subsequent calculations. It was found that the optimised fit was considerably improved by augmenting the set of optimisation variables to include the heater length, which is used in the calculation of the power applied per unit thickness of sediment, $Q'$, from the total power input. Sensitivity to the effective length of the heater is probably caused by the application of the two-dimensional model, described by Eqs. (4)–(7), to an experimental set up that allows some loss of heat in the third dimension. The optimised heater length of 3.1 mm (reduced from a physical length of 3.5 mm) was then used in all subsequent calculations. It is implicitly assumed, therefore, that the dependence of this effective heater length on the thermal properties of the embedding medium is small enough for the value determined in agar to be applicable in the saturated sand of subsequent experiments. The results of one agar experiment and the model fit is shown in Fig. 4.

### Estimation of specific discharge and flow direction

Initially, optimisation was carried out for all experiments with a given probe orientation, by constraining the volumetric heat capacity and the thermal diffusivity to apply to each flow measurement but allowing values of the thermal advective term and flow orientation to vary between measurements. The longitudinal and transverse dispersivity values were held constant at 0.0001 m and 0.00001 m, respectively, following some initial investigations that showed little sensitivity of the specific discharge vector to realistic dispersivity values. A second set of optimisations was conducted, with improved results, in which the volumetric heat capacity was also allowed to vary between measurements, but its value, averaged over all the flow measurements for a given probe orientation, was used in Eq. (8) to estimate flow rate. Because of the improved quality of the results, this strategy was adopted for all estimates, including those reported below. This improvement appears to be related to the simplifying assumptions that have been made in the development of the mathematical model of the probe behaviour. The heater occupies approximately 14% of the distance
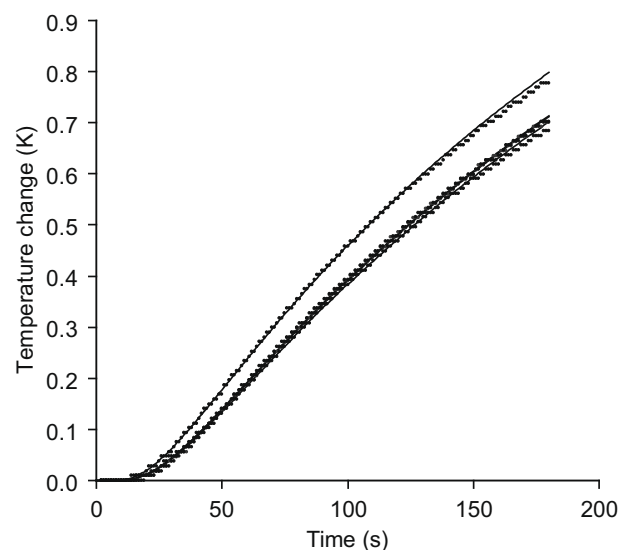


**Fig. 4.** Changes in temperature in an experiment with zero flow in an agar gel: experimental (dots) asnd modelled (solid lines). The results for the North, South and East sensors are almost indistinguishable, but those for the West sensor show an additional distinctive rise. The optimisation RMS error = 0.0055 K.

from its centre to that of a sensor, but the model is based upon the assumption that it has negligible diameter, and so ignores its thermal properties and effect on water flow. Thus, in the context of Eqs. (3)–(7), $(\rho C)_m$ should be thought of as an effective parameter describing the heat capacity of the composite system of sediment and heater and, since the cooling of the heater will be a function of the water flow around it, may be flow rate dependent. In the mathematical model used here, the effect of the heat source is encapsulated in the constant term, $T_0$, given in Eq. (3), which is the only place that $(\rho C)_m$ appears explicitly. In practice, $T_0$ was used as an optimisation parameter in place of $(\rho C)_m$, which was then calculated from Eq. (3). However, in converting the thermal advective parameter to specific discharge (Eq. (8)) the true value of the heat capacity is required. It is implicit in the method adopted that the true heat capacity is sufficiently well approximated by the mean of the effective values derived through optimisation. The improvement in accuracy seen in this approach lends support to this assumption. An additional advantage is that the mean heat capacity can be calculated easily from successive applications of the device in the field, producing an increasingly robust estimate of this parameter with time.

Fig. 5 illustrates the typical model fit to data achieved for just a single flow measurement. Roughly speaking, the total spread of the temperature changes is related to the magnitude of the specific discharge, and the separation between sensor responses provides information on the flow direction.

Fig. 6 shows the magnitude and direction of the optimised specific discharge from the full suite of experiments in the sand column. Table 1 summarises the RMS error achieved in the optimisation for each set of experiments and the associated estimates of the thermal diffusivity of the saturated sediment and the effective heat capacity.

The estimates of non-zero specific discharge are generally good, but with some erratic values. The estimates in the case of zero flow indicate that the sensitivity of the probe in determining the magnitude of specific discharge is poor for some flows less than 1 md$^{-1}$. Table 2 summarises the errors (estimated minus actual value) as a function of specific discharge. These error statistics are based upon just four values and should be interpreted with caution. In particular, the standard deviation of the errors from such
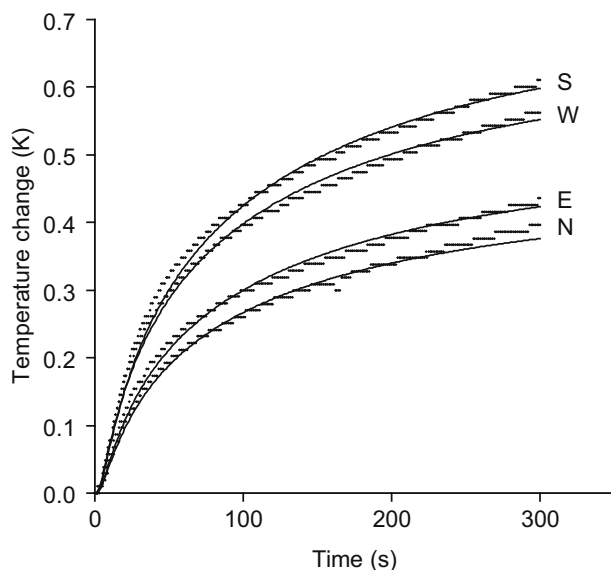
a small sample is subject to a high level of uncertainty. Errors of estimation are discussed more fully in "Errors".

The estimates of the flow direction are generally very good, with all but one estimate being within ±10° of the correct value, 14 out of the 20 estimates being within ±5°, and 5 being within ±1°. Summary statistics of the errors in estimation are given in Table 3. The quality of the estimation tends to decrease at lower flow rates.

Taken across all individual measurements, the estimated effective heat capacity, $(\rho C)_m$, has a mean value of $3.00 \times 10^6$ Jm$^{-3}$ K$^{-1}$ and standard deviation $1.15 \times 10^5$ Jm$^{-3}$ K$^{-1}$. Although this parameter does not represent the heat capacity of the saturated sediment precisely, it is interesting to compare its value with those given for sand in the literature. The porosity weighted arithmetic mean of the fluid and the solid heat capacity, $(\rho C)_s$, is generally taken to be a good estimator of the heat capacity of the mixture (e.g. Ochsner et al., 2001; Ren et al., 2003), which can therefore be estimated by

$$(\rho C)_m = n(\rho C)_f + (1-n)(\rho C)_s \tag{10}$$

where $n$ is the porosity of the sediment.

Published values for sand vary. Cox et al. (1989) give the heat capacity for α-quartz at 20 °C as $41.46 \pm 0.20$ J mol$^{-1}$ K$^{-1}$, which translates to $1.83 \times 10^6$ Jm$^{-3}$ K$^{-1}$. Using a gravimetric estimate of porosity of 33%, this gives a value of the heat capacity of the experimental sand of $2.61 \times 10^6$ Jm$^{-3}$ K$^{-1}$. Ren et al. (2003) give a value for sand grains of $2.41 \times 10^6$ Jm$^{-3}$ K$^{-1}$, which results in a saturated sand heat capacity of $3.00 \times 10^6$ Jm$^{-3}$ K$^{-1}$.

## Discussion

### Errors

The underestimate of the actual flow rate of 3.3 md$^{-1}$ seen in Fig. 6b appears to be related to an instrumental error. The temperature change curve for the North sensor shows an unphysical sharp rise of just under 0.06 K from an apparently stable ambient temperature immediately the heater is turned on. This rise is followed by a brief plateau followed by a more typical temperature change profile, which starts at the same time as the initial rises seen in the other sensors. If the plateau is taken to represent zero change, rerunning the optimisation software produces the improved results shown in Fig. 7. The original flow rate error of −33% is modified to 10%. The directional error merely changes from 2° to −2°. The cause of such an instrumental error is unclear, but illustrates the sensitivity of measurement to device performance.

The significant underestimate at the highest flow rate shown in Fig. 6a is more difficult to explain. Examination of the temperature change curves for the complete range of flow rates in this orientation shows that, contrary to expectation, all the recorded temperature changes increase when the flow rate is raised from 4.4 md$^{-1}$ to 5.6 md$^{-1}$ and their spread decreases. The latter has the dominant effect on the estimated flow rate, leading to a low estimate. Optimisation over truncated versions of the data spanning periods from 1 to 4 min confirms that there is an upward drift in temperatures that increases with time, but that the spread as a function of the length of the data set remains largely the same and hence the estimate of flow rate does not change radically by shortening the data set. It is possible that the drift in temperatures (by about 0.07 K on average after 5 min) is caused by ambient temperature changes during the experiment, but the more significant decreased spread remains unexplained.

There is the suggestion of a bias in the estimated magnitude of the specific discharge in Fig. 6d, the cause of which is uncertain. In this case the flow is orientated at 45° to the N–S axis and it is con-
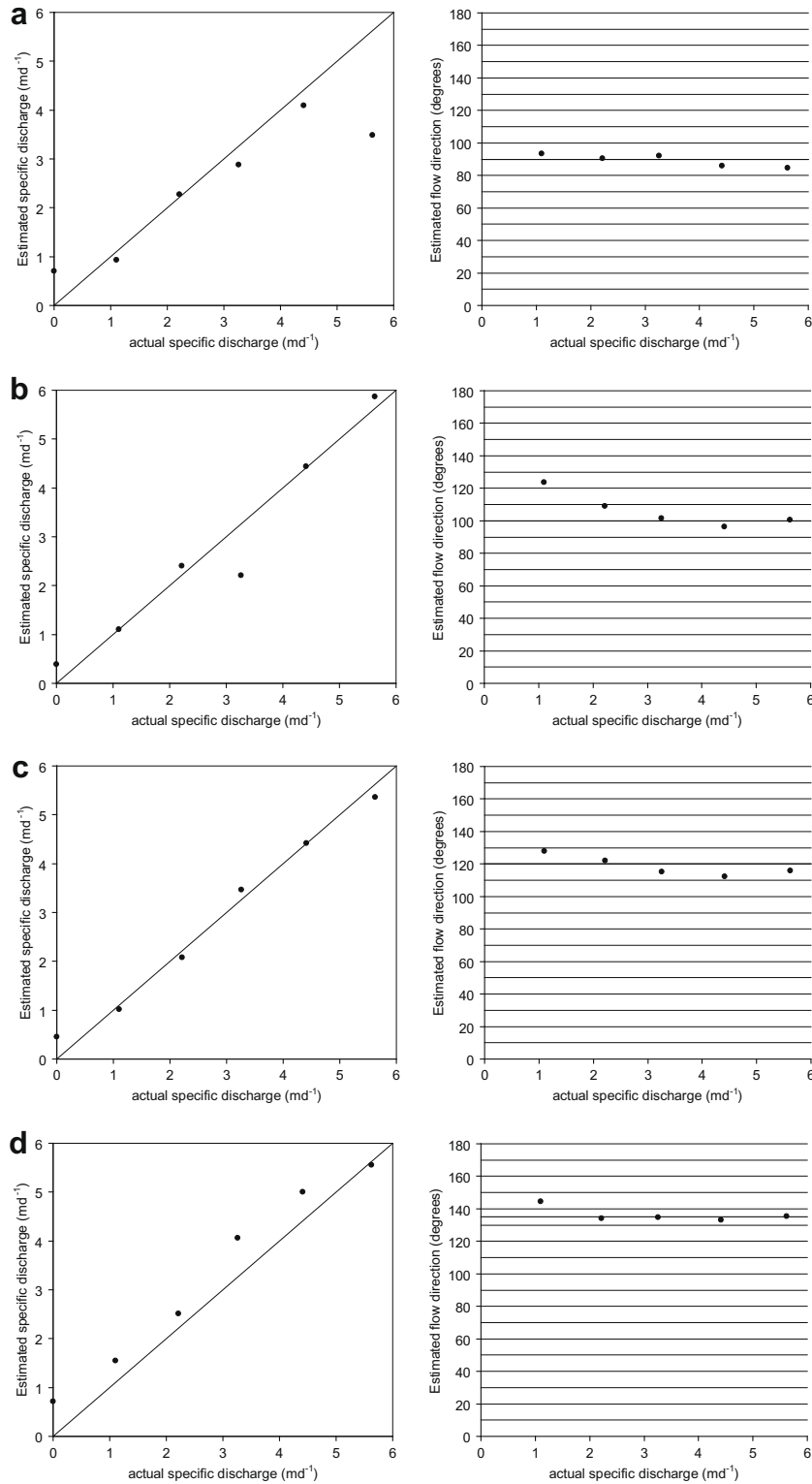


**Fig. 5.** Typical optimised fit (solid lines) to temperature data (dots) for a single flow measurement for flow direction of 120°.

**Fig. 6.** Summary of estimated specific discharge and flow direction for experimental flow directions (measured clockwise from East) of (a) 90° (b) 100° (c) 120° and (d) 135°.

ceivable that the distortion of the flow field caused by the heater and temperature sensors may have some effect on the measurement, which may be worthy of further investigation. It is also possible that the bias results from minor misalignments or tangential displacements of the temperature sensors not accounted for in the estimation of the effective radial distances between the heater and sensors ("Effective distances between the heater and sensors"). It is noted, however, that the consistent bias seen in some previous

studies (see Introduction) was not apparent in the results obtained here.

*Estimation of specific discharge at low flow rates*

As noted in "Solutions of the heat balance equation", the model underlying the parameter optimisation routine is not applicable when the specific discharge is zero since under these conditions a

**Table 1**
Summary of estimated thermal parameters.

| Flow direction | 90° | 100° | 120° | 135° |
|---|---|---|---|---|
| RMS error (K) | 0.0104 | 0.0112 | 0.0097 | 0.0090 |
| Thermal diffusivity, $\lambda$ (m$^2$ s$^{-1}$) | $1.06 \times 10^{-6}$ | $9.87 \times 10^{-7}$ | $1.01 \times 10^{-6}$ | $1.17 \times 10^{-6}$ |
| Volumetric heat capacity, $(\rho C)_m$ (Jm$^{-3}$ K$^{-1}$) | $3.05 \times 10^{6}$ | $3.03 \times 10^{6}$ | $2.98 \times 10^{6}$ | $2.95 \times 10^{6}$ |

Directions measured clockwise from East.

**Table 2**
Error statistics for estimated specific discharge.

| Experimental specific discharge (md$^{-1}$) | Mean error (md$^{-1}$) | Standard deviation of error (md$^{-1}$) | Mean relative error |
|---|---|---|---|
| 0.00 | 0.562 | 0.168 | |
| 1.10 | −0.042 | 0.265 | 0.038 |
| 2.21 | 0.113 | 0.204 | 0.051 |
| 3.26 | 0.103 | 0.800 | 0.032 |
| 4.41 | 0.076 | 0.363 | 0.017 |
| 5.62 | −0.563 | 1.066 | −0.100 |

**Table 3**
Error statistics for estimated flow direction.

| Experimental specific discharge (md$^{-1}$) | Mean error (°) | Standard deviation of error (°) |
|---|---|---|
| 1.10 | 11.2 | 8.8 |
| 2.21 | 2.6 | 4.4 |
| 3.26 | −0.4 | 3.1 |
| 4.41 | −4.3 | 2.4 |
| 5.62 | −2.2 | 3.0 |

direction of flow is not meaningful. In fact the sensitivity of the optimised fit to the flow direction, as measured by the derivative of the RMS error with respect to $\theta$, theoretically approaches zero as the flow rate decreases. This can be seen in practice in Fig. 8, which shows how the RMS error changes with deviations from the optimum value of $\theta$ and with specific discharge. Note that the curve for $q = 0$ is almost indistinguishable from the horizontal axis.

This insensitivity has two important implications. First, the quality of the estimate of the flow direction tends to decrease as the flow rate becomes small. Second, the quality of the direction estimate affects the estimate of flow rate. Consider, for example, the extreme case of zero flow. If there is any discrepancy between the actual positions of the probe elements and those required by the mathematical model describing heat flow, the application of the optimisation routine will produce a value of $\theta$ that is deter-

mined solely by the geometry of the probe, and which will lead to the introduction of a fictitious, non-zero value of $u$ in order to minimise the RMS error. The effect of these fictitious values can be seen clearly in Fig. 6.

A major challenge for the heat perturbation method is to distinguish between valid estimates of reasonably low flow rates and those produced artificially by very low flows. A way forward might be through investigation of the sensitivity of the RMS error to $\theta$, which is simple to calculate, and which has been seen to vary monotonically with flow rate for specific discharges less than 2 md$^{-1}$ in all the experiments reported here.

*Areas of applicability*

The low flow limit of approximately 0.7 md$^{-1}$ reported by Ren et al. (2000) is typical of one-dimensional heat perturbation devices, and "Estimation of specific discharge at low flow rates" highlights a theoretical limitation to the identification of near-zero flows in a two-dimensional system. Thus, at present, the use of heat perturbation devices to measure saturated zone flows is restricted to areas of concentrated groundwater flow where fluxes are higher than in most regional contexts. Such locations may include riparian areas, where flows have been shown to be highly variable and potentially large locally (e.g. Lamontagne et al., 2002; Cardenas et al., 2004; Smith, 2005; Warren et al., 2005; Cardenas and Wilson, 2007; Keery et al., 2007), coastal areas (e.g. Paulsen et al., 2001, who record submarine groundwater discharges in one dimension in excess of 2.8 md$^{-1}$ using an ultrasonic flow meter; and Lamontagne et al., 2002, who measure groundwater flows in an estuarine area up to 9.6 md$^{-1}$ using point dilution techniques) or where flows are significantly affected by engineering works or built structures. In addition, areas with macropore flow may exhibit particularly high discharges that are difficult to measure directly with large scale measuring devices due to their destructive methods of installation (e.g. Mosley, 1979 and Elçi and Molz, 2008, who use tracer test data and modelling to infer specific discharges in a riparian wetland as large as 100 md$^{-1}$). Reviews of hyporheic zone flow monitoring methods include those of Greswell (2005) and Kalbus et al. (2006).
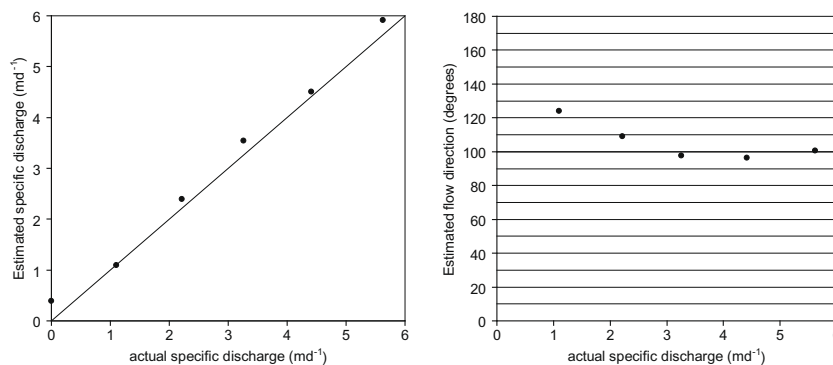


**Fig. 7.** Optimised fit of the model to data for flow at 100° clockwise from East (Fig. 6b) after shifting the temperature change curve for the North sensor down by 0.06 K.
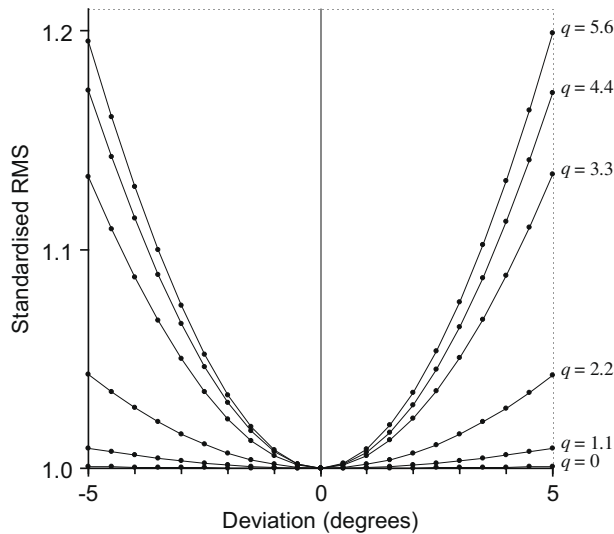
**Fig. 8.** Sensitivity of the model fit for the 120° flow direction as a function of deviation from the optimised flow direction and specific discharge, $q$ (md$^{-1}$). The RMS optimisation error is standardised by the RMS error for the optimised value of $\theta$.

### Potential methods of field installation

Field trials have yet to be conducted, but there are several installation methods that might be envisaged. In suitably soft sediments, the probe might be pushed directly into the substrate on the end of a spear, which could then be withdrawn to leave the probe in place for long-term deployment or withdrawn with the probe attached for single measurements. In more consolidated sediments or those containing larger grains, it would be possible to use a 'lost-point' technique, as shown in Fig. 9. The probe is driven into the sediment using a tube and sacrificial drive point, both of which protect the probe until it has been placed at the required depth. The drive tube and probe are then withdrawn leaving the drive point in place. At this stage the release mechanism attaching
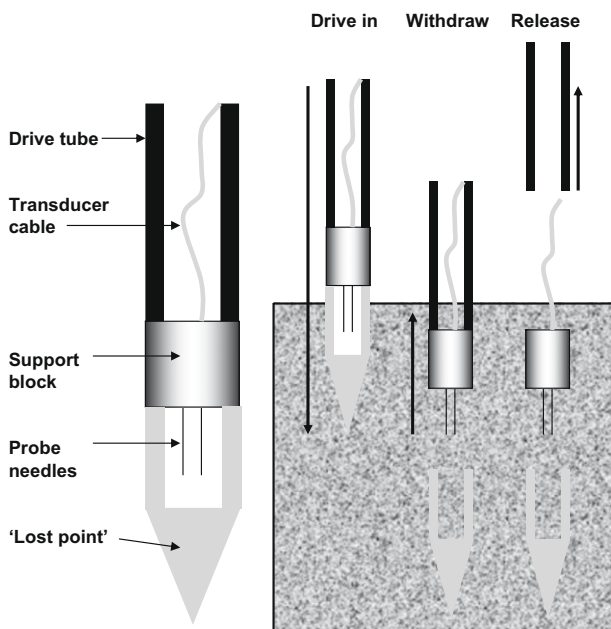
the probe to the drive tube is activated and the drive tube withdrawn further leaving the probe in place.

### Conclusions

A prototype device for monitoring the magnitude and direction of groundwater specific discharge at a point in a two-dimensional flow system has been constructed and has undergone testing in the laboratory. The results of the tests indicate that the heat perturbation principle upon which the device is based is suitable for determining the magnitude of specific discharge to a degree of accuracy that would be useful in practical applications in soft sediments in dynamic groundwater zones, and that its direction can generally be determined to a high level of precision. Concomitant estimates of the volumetric specific heat capacity of the saturated sand used in the experiment compare well with published values for similar sediments. No systematic underestimation of flow is observed.

The prototype device was inexpensive to construct (around 100 GBP for the components, support block and controller) and has a low enough energy requirement (approximately 65 J per measurement in tests) to be powered by a battery such as a small 1.2 Ah, 12 V sealed lead acid type. The laboratory tests were conducted manually, but it is perfectly feasible that the device could incorporate small-scale control and logging equipment that would allow measurements to be taken automatically in the field over an extensive period, with data stored for intermittent downloading and subsequent off-site processing. Thus, in principle, a heat perturbation device could be suitable for deployment at multiple locations in the field, including in remote areas. The size of the device minimises the possibility of the detection of anomalous vertical flows reported for larger devices (e.g. Su et al., 2006), and combined with its relatively low cost, allows the spatial as well as the temporal variability of specific discharge to be assessed.

The accuracy and reliability of the estimates of the groundwater specific discharge vector have been shown to depend strongly upon the geometrical precision of manufacture and the quality of the temperature monitoring system. These factors become most significant in the estimation of low flows. The device described here is a basic prototype, built with the purpose of assessing the suitability of the heat perturbation method for determining the magnitude and direction of specific discharge in principle. Further investigation of the lower detection limit of the device needs to be conducted, but requires the construction of a second prototype, manufactured to tighter geometrical tolerances and including higher resolution temperature measurement. Preliminary modelling has shown that estimates are insensitive to dispersivity values appropriate to the scale of the device.

The device is intended primarily for small scale, intensive monitoring programmes rather than for measuring regional groundwater flows. Indeed, the evidence from the experiments described here suggests that it would be inappropriate to use it in the latter context due to the uncertain accuracy at low specific discharges. Although inconclusive, the evidence suggests that the combination of the device and the optimisation method of analysis described here is unlikely to produce accurate results for the magnitude of specific discharge below around 0.5 md$^{-1}$.

It is expected that the robustness of specific discharge estimates will increase with time in the field as more measurements contribute to estimation of system constants such as the thermal properties of the saturated sediment.



**Fig. 9.** Overview of a possible method of installation using a sacrificial drive point.

## References

Ballard, S., 1996. The in situ permeable flow sensor: a ground-water flow velocity meter. Ground Water 34 (2), 231–240.

Basinger, J.M., Kluitenberg, G.J., Ham, J.M., Frank, J.M., Barnes, P.L., Kirkham, M.B., 2003. Laboratory evaluation of the dual-probe heat-pulse method for measuring soil water content. Vadose Zone J. 2, 389–399.

Bear, J., 1979. Hydraulics of Groundwater. McGraw-Hill.

Bristow, K.L., 1998. Measurement of thermal properties and water content of unsaturated sandy soil using dual-probe heat-pulse probes. Agric. Forest Meteorol. 89, 75–84.

Campbell, G.S., Calissendorff, C., Williams, J.H., 1991. Probe for measuring soil specific heat using a heat-pulse method. Soil Sci. Soc. Am. J. 55, 291–293.

Cardenas, M.B., Wilson, J.L., Zlotnik, V.A., 2004. Impact of heterogeneity, bed forms, and stream curvature on subchannel hyporheic exchange. Water Resour. Res. 40, W08307. doi:10.1029/2004WR003008.

Cardenas, M.B., Wilson, J.L., 2007. Exchange across a sediment–water interface with ambient groundwater discharge. J. Hydrol. 346, 69–80.

Carslaw, H.S., Jaeger, J.C., 1959. Conduction of Heat in Solids, second ed. Oxford University Press.

Cox, J.D., Wagman, D.D., Medvedev, V.A., 1989. CODATA Key Values for Thermodynamics. Hemisphere Publishing Corp., New York.

Dudgeon, C.R., Green, M.J., Smedmoor, W.J., 1975. Heat-pulse flowmeter for boreholes. Technical Report No. 4. Water Research Centre, Medmenham, UK.

Elçi, A., Molz, F.J., 2008. Identification of lateral macropore flow in a forested riparian wetland through numerical simulation of a subsurface tracer experiment. Water Air Soil Pollut. doi:10.1007/s11270-008-9798-5.

Gao, J., Ren, T., Gong, Y., 2006. Correcting wall flow effect improves the heat-pulse technique for determining water flux in saturated soils. Soil Sci. Soc. Am. J. 70, 711–717.

Greswell, R.B., 2005. High-resolution in-situ monitoring of flow between aquifers and surface waters. Environment Agency Science Report SC030155/SR4. Environment Agency, Bristol.

Guaraglia, D.O., Pousa, J.L., 2007. A method to improve flow-velocity measurements from an array of partially cosine response sensors. IEEE Trans. Instrument. Measure. 56 (5), 1721–1724.

Ham, J.M., Benson, E.J., 2004. On the construction and calibration of dual-probe heat capacity sensors. Soil Sci. Soc. Am. J. 68, 1185–1190.

Heitman, J.L., Basinger, J.M., Kluitenberg, G.J., Ham, J.M., Frank, J.M., Barnes, P.L., 2003. Field evaluation of the dual-probe heat-pulse method for measuring soil water content. Vadose Zone J. 2, 552–560.

Hopmans, J.W., Šimunek, J., Bristow, K.L., 2002. Indirect estimation of soil thermal properties and water flux using heat pulse probe measurements: geometry and dispersion effects. Water Resour. Res. 38 (1), 45–56. doi:10.1029/2000WR000071.

Kalbus, E., Reinstorf, F., Schirmer, M., 2006. Measuring methods for groundwater–surface water interactions: a review. Hydrol. Earth Syst. Sci. 10, 873–887.

Keery, J., Binley, A., Crook, N., Smith, J.W.N., 2007. Temporal and spatial variability of groundwater–surface water fluxes: development and application of an analytical method using temperature time series. J. Hydrol. 336, 1–16.

Knight, J.H., Kluitenberg, G.J., 2004. Simplified computational approach for dual-probe heat-pulse method. Soil Sci. Soc. Am. J. 68, 447–449.

Lamontagne, S., Dighton, J., Ullman, W., 2002. Estimation of groundwater velocity in riparian zones using point dilution tests. CSIRO Land and Water. Technical Report 14/02, 16pp.

Mori, Y., Hopmans, J.W., Mortensen, A.P., Kluitenberg, G.J., 2003. Multi-functional heat pulse probe for the simultaneous measurement of soil water content, solute concentration, and heat transport parameters. Vadose Zone J. 2, 561–571.

Mosley, M.P., 1979. Streamflow generation ion a forested watershed, New Zealand. Water Resour. Res. 15 (4), 795–806.

Ochsner, T.E., Horton, R., Kluitenberg, G.J., Wang, Q., 2005. Evaluation of the heat pulse ratio method for measuring soil water flux. Soil Sci. Soc. Am. J. 69, 757–765.

Ochsner, T.E., Horton, R., Ren, T., 2001. A new engineers perspective on soil thermal properties. Soil Sci. Soc. Am. J. 65, 1641–1647.

Paulsen, R.J., Smith, C.F., O'Rourke, D.O., Wong, T.-F., 2001. Development and evaluation of an ultrasonic ground water seepage meter. Ground Water 39 (6), 904–911.

Perry, R.H., Green, D.W., 1997. Perry's Chemical Engineers' Handbook, seventh ed. McGraw-Hill.

Ren, T., Kluitenberg, G.J., Horton, R., 2000. Determining soil water flux and pore water velocity by a heat pulse technique. Soil Sci. Soc. Am. J. 67, 552–560.

Ren, T., Noborio, K., Horton, R., 1999. Measuring soil water content, electrical conductivity, and thermal properties with a thermo-time domain reflectometry probe. Soil Sci. Soc. Am. J. 63 (3), 457–459.

Ren, T., Ochsner, T.E., Horton, R., Ju, Z., 2003. Heat-pulse method for soil water content measurement: influence of the specific heat of the soil solids. Soil Sci. Soc. Am. J. 67, 1631–1634.

Smith, J.W.N., 2005. Groundwater–surface water interactions in the hyporheic zone. Environment Agency Science Report SC030155/1. Environment Agency, Bristol, UK.

Su, G.W., Freifeld, B.M., Oldenburg, C.M., Jordan, P.D., Daley, P.F., 2006. Interpreting velocities from heat-based flow sensors by numerical simulation. Ground Water 44 (3), 386–393.

Wang, Q., Ochsner, T.E., Horton, R., 2002. Mathematical analysis of heat pulse signals for soil water flux determination. Water Resour. Res. 38 (6). doi:10.1029/2001WR001089.

Warren, D.R., Sebestyen, S.D., Josephson, D.C., Lepak, J.M., Kraft, C.E., 2005. Acidic groundwater discharge and in situ egg survival in Redds of lake-spawning brook trout. Trans. Am. Fish. Soc. 134, 1193–1201.

Welch, S.M., Kluitenberg, G.J., Bristow, K.L., 1996. Rapid numerical estimation of soil thermal properties for a broad class of heat-pulse emitter geometries. Measure. Sci. Technol. 7, 932–938.

Wilson, J.T., Mandell, W.A., Paillet, F.L., Bayless, E.R., Hanson, R.T., Kearl, P.M., Kerfoot, W.B., Newhouse, M.W., Pedler, W.H., 2001. An evaluation of bore-hole flowmeters used to measure horizontal ground-water flow in limestones of Indiana, Kentucky, and Tennessee, 1999. USGS Water Resources Investigations Report 01-4139. US Department of the Interior and USGS, Indianapolis, Indiana.